

Compression of SAR complex image with wavelet transform block adaptive vector quantization

DING Hong, YI Hang, WANG Guang-xue, HUANG Xiao-tao

College of Electronic Science and Engineering, National University of Defense Technology, Hunan Changsha 410073 China

Abstract: With the development of high-resolution SAR systems, it is necessary to develop image compression techniques to compress these products because the volume of data in SAR systems is increasing rapidly. Unlike the compression of SAR real images, the compression of SAR complex images usually needs to keep the phase information which is a difficulty task. In this paper, the correlation of complex SAR images data before and after the wavelet transform is analyzed. Then the theory and methodology of a wavelet-based compressing method for SAR complex images, the Wavelet Transform Block Adaptive Vector Quantization (WT-BAVQ) algorithm, is presented. At the same time, as the compression is performed to a SAR complex image with WT-BAVQ, the Average Spatial Correlation (ASC) and Average Phase Correlation Coefficient (APCC) are achieved and the decompressed image is given. Moreover, the comparison of ASC and APCC is made with Block Adaptive Vector Quantization (BAVQ), Wavelet Transform Vector Quantization (WT-VQ) and wavelet transform block adaptive quantization (WT-BAQ). The experiments manifest that with the same compression ratio, the ASC of WT-BAVQ is higher than that of the other three algorithms.

Key words: SAR complex image, wavelet transform, block adaptive quantization, vector quantization

CLC number: TP722.6/TP751.1

Document code: A

Citation format: Ding H, Yi H, Wang G X and Huang X T. 2010. Compression of SAR complex image with wavelet transform block adaptive vector quantization. *Journal of Remote Sensing*. 14(1): 033—042

1 INTRODUCTION

With the development of high-resolution SAR systems, it is necessary to develop image compression techniques to compress these products in order to transmit them in real-time, because the volume of data in SAR systems is increasing rapidly. There are three compression classes for SAR data: compression of SAR raw data, compression of SAR complex images and compression of magnitudes of SAR image.

SAR complex images, which are different from the optical images, have three attributes. Firstly, they are complex, with phase as well as magnitude. Secondly, they possess greatly high dynamic range. Thirdly, they have abundant veins. Consequently, image compression methodologies that offer good performances on optical images generally do not produce acceptable performance on SAR complex images. Historically, the phase components of SAR images have been discarded. Recently, several powerful new techniques relying on the full complex nature of the imagery have generated, including autofocus and interferometry. Therefore the compression of SAR complex images is of great necessity.

Up to now, only a few algorithms exist in compressing com-

plex SAR images, and they are mainly transform-based image compression techniques, such as algorithms based on frequency domain (Eichel & Ives, 1999) and wavelet domain (Werness *et al.*, 1994; Brandfass *et al.*, 1997; Ives *et al.*, 1998; Zeng & Cumming, 2001). The complexity of the former is lower than the latter, but the performance is not as good as the latter.

Considering the coefficients of real and imaginary part of SAR complex images are more correlated after the wavelet transform is used, we separate the complex SAR images into real and imaginary parts. First, we carry out wavelet transform to the real and imaginary part. Then vector quantization to the wavelet transform results are performed separately. Since the real and imaginary part of SAR complex images both have a approximate Gaussian distribution which is still a Gaussian distribution after a linear transformation, we quantized the wavelet coefficients of the real and imaginary part using a block adaptive quantizer separately before the vector quantization. In this way, a discrete Gauss distribution which have N magnitudes (N is decided by quantization bits) is attained (Qin *et al.*, 2005). The data of the whole transmitting system have the same standard deviation. As a result, it can save the encoding time because only one codebook which is independent of the data system is needed in vector quantization.

Received: 2008-10-24; **Accepted:** 2009-04-01

Foundation: Program for New Century Excellent Talents in University (No.NCET-07-0223)

First author biography: DING Hong (1973—), female, instructor. She received M.S degree in electrical engineering from National University of Defence Technology. Her research interests include signal detection and estimation, SAR data processing and wireless communication. She has published about 10 papers and 1 book. E-mail: dh1nudt@tom.com

2 WAVELET ANALYSIS OF SAR COMPLEX IMAGES

For a data block whose size is $M \times N$, as the interval of row is k , the correlation coefficient is:

$$\rho = \frac{\sum_{j=1}^N \sum_{i=1}^M [(X(i, j) - m) \times (X(i+k, j) - m)]}{\sqrt{\sum_{j=1}^N \sum_{i=1}^M (X(i, j) - m)^2} \times \sqrt{\sum_{j=1}^N \sum_{i=1}^M (X(i+k, j) - m)^2}} \quad (1)$$

where, m is the mean of $X(i, j)$. When the interval of array is k , the correlation coefficient is:

$$\rho = \frac{\sum_{i=1}^M \sum_{j=1}^N [(X(i, j) - m) \times (X(i, j+k) - m)]}{\sqrt{\sum_{i=1}^M \sum_{j=1}^N (X(i, j) - m)^2} \times \sqrt{\sum_{i=1}^M \sum_{j=1}^N (X(i, j+k) - m)^2}} \quad (2)$$

where, m is the mean of $X(i, j)$.

The change of ρ before and after the wavelet transform of two different SAR complex images can be analyzed. Image 1, whose magnitude map is shown in Fig. 1, is a P-band complex SAR image. The number of sampling points at direction of azimuth and range are both 1024. After three decomposition

iterations to the coefficients of real and imaginary part of Image 1 by using the biorthogonal Daubechies 9/7 wavelet filter (Wang & Yuan, 2001), they both yield 10 sub-bands which are LL3, LH3, HL3, HH3, LH2, HL2, HH2, LH1, HL1 and HH1. Using the definition of Eq.(1) and Eq.(2), we compute ρ of coefficients before and after the discrete wavelet transform. The simulation results which are performed in MATLAB are shown in Fig. 2. Processing a Ku-band complex image whose magnitude map is shown in Section 6, and the simulation results are shown in Fig. 3. As the figures show, we can see that ρ of the coefficients is bigger after the wavelet transform is performed, and enhancement is different for different images.

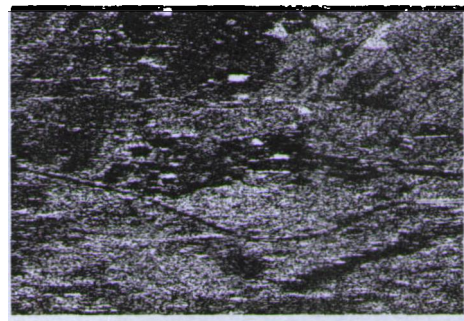


Fig. 1 Complex Image 1

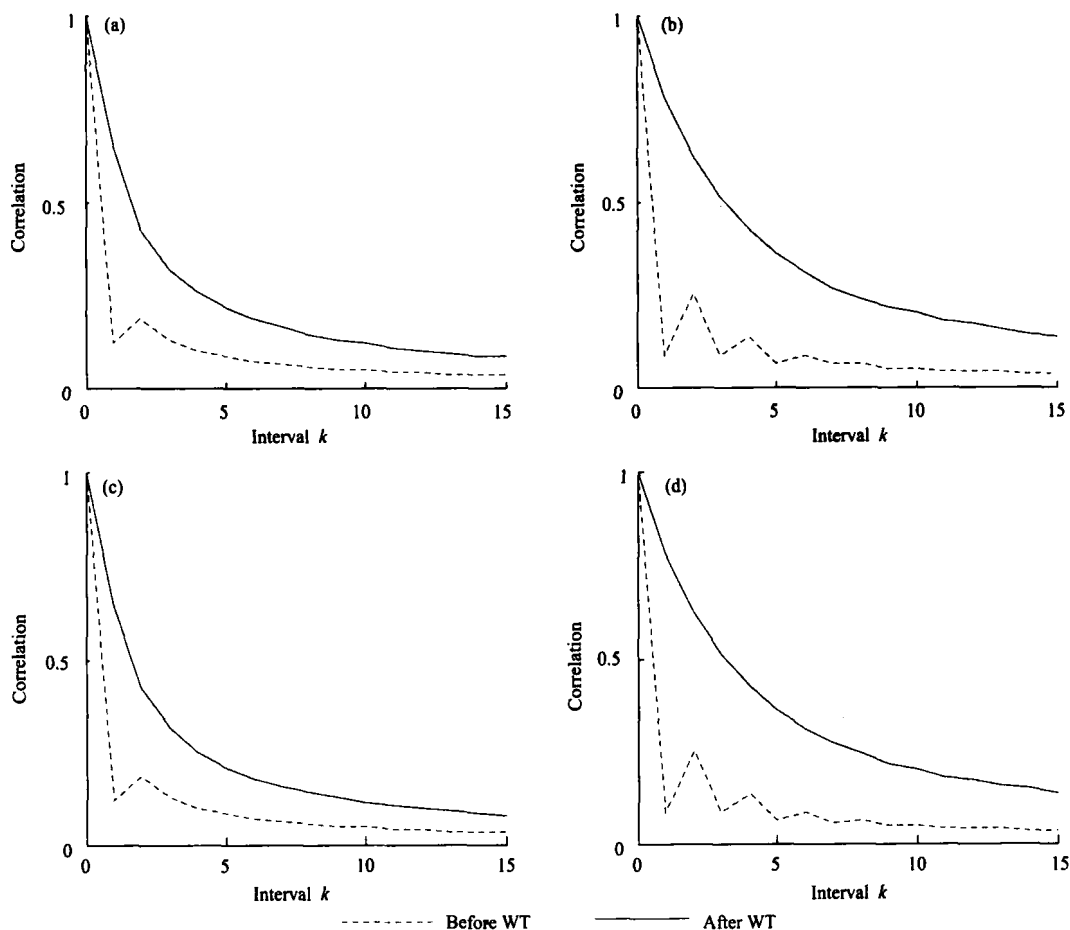


Fig. 2 Comparison of correlation coefficient of Image 1

(a) Correlation in azimuth of real part; (b) Correlation in range of real part; (c) Correlation in azimuth of imaginary part; (d) Correlation in range of imaginary part

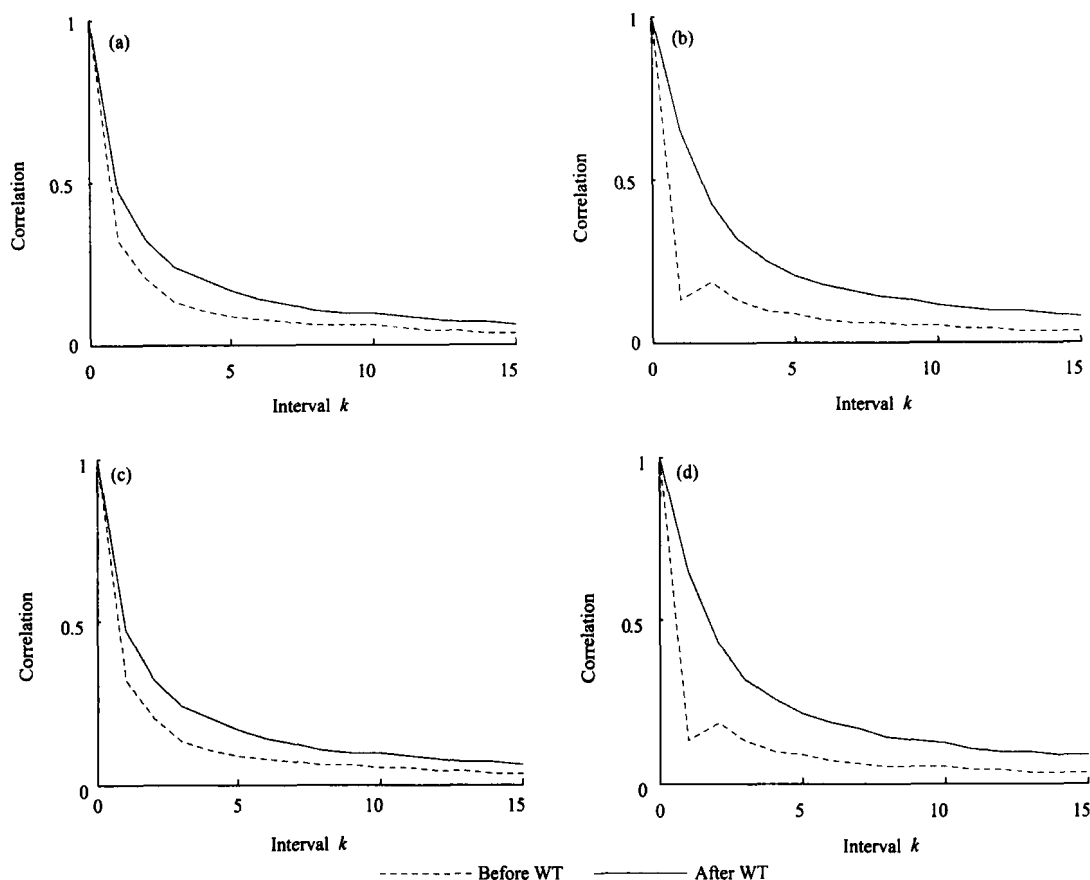


Fig. 3 Comparison of correlation coefficient of Image 2

(a) Correlation in azimuth of real part; (b) Correlation in range of real part; (c) Correlation in azimuth of imaginary part; (d) Correlation in range of imaginary part

3 BLOCK ADAPTIVE QUANTIZATION ON WAVELET COEFFICIENTS

The real and imaginary parts of SAR complex images are signals. Moreover, they have probability distributions close to the Gaussian distribution. If a linear transform is performed to an approximately Gaussian distribution signal, it is still an approximately Gaussian distribution signal. In this paper, we use a Block Adaptive Quantizer (Kwok & Johnson, 1989) to the wavelet transformed results which are approximately Gaussian distribution signals. The block size is 32×32 . First, we make the mean 0 and the variation 1 by doing standardization to each block. Then perform 4 bit quantization to the standard normal distribution data according the L-M algorithm. After this step, we get signals with normal distribution which has 16 magnitudes. As a result, it can make vector quantization more expediently. Because after BAQ to data of different images, the signals we get have the same probability distribution. Then when the vector quantizer is used on the data of different images, the codebook needed is the same. It can save the compression time efficiently.

4 VECTOR QUANTIZATION

The performance of a vector quantizer (Linde *et al.*, 1980) is better when the input vectors are more correlated to each other. As it is demonstrated before, ρ of the coefficients gets bigger

after wavelet transform is used. This result can improve the performance of vector quantization at a certain extent. Moreover, vector conformation of the wavelet coefficients which are to be quantized is also very important. It can not only decide whether the complexity of vector quantization can be lower, but also can effect the performance.

4.1 Vector conformation of wavelet coefficients

In this paper, we apply the method which is mentioned by Chen (2002) to finish the vector conformation. After performing the wavelet transform, sub-images are isomorphic to each other. This comparability does not only exist in the sub-images which are in the same scale, but also exists between different scales. Besides, the comparability is highest among the corresponding sub-bands which are in different scales. To improve the efficiency of a vector quantizer, we must utilize the correlation sufficiently when we construct vectors. It is an effective way to put isomorphic pixels of sub-band images into the same vector. Considering that the information of high-frequency sub-bands play an important role in improving the quality of reconstructed images, the high-frequency sub-bands coefficients must be included in vector conformation. In addition, for the sake of avoiding the scalar quantization to the low-frequency coefficients, we put them together with the corresponding high-frequency coefficients in a same vector. According to this idea, we put the data which are in the same location of sub-images of different scales together to form a tree

structure which is shown in Fig. 4. In this way, we can use one codebook for the whole image. Fig. 4 shows the three-level wavelet decomposition results which have ten sub-bands. We pick up 1, 4 and 16 coefficients from each level separately. As a result, we get 64-D vectors. Vectors with lower dimensions are extracted from the 64-D vectors by nonlinear interpolative techniques in references. But in this paper, we perform vector quantization to the 64-D vectors because the energy of complex SAR images are not concentrated distributed.

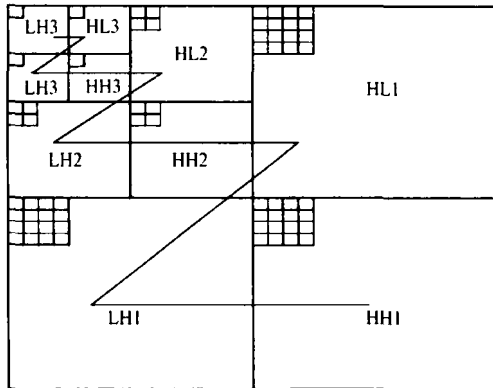


Fig. 4 Vector conformation

4.2 Generation of codebook

When the input source of vector quantizer has a uniform distribution, we can get the optimal codebook by applying the equal-probability principle. But if they are with arbitrary probability distributions, we can obtain the optimal codebook only by using the equal-distortion principle. Obviously, the probability distribution of input source in this paper is not uniform. Therefore we adopt the Minimax Partial Distortion Competitive Learning algorithm (Li & Jiang, 2004) to generate the codebook.

4.3 Encoding algorithm

A fast encoding algorithm is got by utilizing characteristics of distance between input vectors and the codewords, characteristics of distance between codewords and partial-distortion elimination criterion. It computes the sum of every codeword in codebook C . And then generates ordered codebook C_s by arranging them based on the ascending order of the sum of their vector components. The sums are also saved in the codebook C_s . For every input vector, computing the sum and obtain the tentative matching codeword. Then search is performed up and down iteratively (Pan *et al.*, 2003) and finish the encoding process using rules of the fast algorithm.

5 QUALITY METRIC

In this paper, the Complex Spatial Correlation Coefficient (Robert *et al.*, 1999) is used to evaluate the performance of the WT-BAVQ compression technique.

The definition of CSCC is:

$$c(x, y) = \frac{\left| \sum_i \sum_j f(i, j) \cdot g^*(i, j) \right|}{\sqrt{\sum_i \sum_j \|f(i, j)\|^2 \cdot \sum_i \sum_j \|g(i, j)\|^2}} \quad (3)$$

where the indices i and j represent pixels in a neighborhood area of pixel (x, y) respectively. The value of CSCC which computed from Eq. (3) is in the range of $[0, 1]$. If every complex value of the original image is equal to the decompressed image in the neighborhood area, the CSCC of this pixel is 1.0. It denotes that the two images are totally correlated in this pixel. When the value of CSCC is 0, it means that two images are not correlated to each other at all. For complex SAR images, this hypothesis is correct when the size of the neighborhood is big enough. We choose the size of the neighborhood 5×5 in this paper. After computing the CSCC to every pixel, we can get an intuitive evaluation of decompressed image quality comparing to the original image on a local scale. If the CSCC is bigger, the two images are more alike to each other. Computing the average of CSCC over the entire image with size $M \times N$, we get the Average Spatial Correlation:

$$ASC = \frac{1}{MN} \sum_x \sum_y c(x, y) \quad (4)$$

The ASC provides the extent of comparability of the entire images, which can be used to evaluate the quality of the reconstructed image on a global scale.

It is important to keep the phase information for the compression of SAR complex images. The Average Phase Correlation Coefficient is used in this paper to analyze the ability of keeping phase information of the entire image. According to the definition of Average Spatial Correlation, we define the Average Phase Correlation Coefficient as:

$$APCC = \frac{1}{MN} \sum_x \sum_y \frac{\left| \sum_i \sum_j f_p(i, j) \cdot g_p^*(i, j) \right|}{\sqrt{\sum_i \sum_j \|f_p(i, j)\|^2 \cdot \sum_i \sum_j \|g_p(i, j)\|^2}} \quad (5)$$

where $f_p(i, j)$ and $g_p(i, j)$ represent the phase in pixel (x, y) of the original and the reconstructed images separately.

6 EXPERIMENTAL RESULTS AND ANALYSIS

The tested image is a Ku-band complex SAR image whose magnitude map is shown in Fig. 5(a). The sampling points of azimuth and range direction are both 1024. Four compression algorithms BAVQ, WT-VQ, WT-BAQ and WT-BAVQ are performed to this image respectively. The environment of these experiments is: CPU: 2GHz; memory: 2G; operation system: Windows XP. The programs are run in IDL 6.3. Table 1 gives the ASC, APCC and run-time of the four techniques. The codebook size of BAVQ, WT-VQ and WT-BAVQ are 256. That is to say, the Compression Ratio (CR) is 64. The dimension of the input vectors is 64. The training vectors which are used in generating codebook are chosen from the input vectors and the length of the training vectors is 1/8 of the total length. The

BAQ step of BAVQ and WT-BAVQ both perform four bit L-M quantization while two bit L-M quantization (CR=4) is used in WT-BAQ. From Table 1, we know that WT-BAVQ obtains the best performance. It has the same CR as WT-VQ and BAVQ, but it produces the biggest ASC and APCC. Besides, run-time of WT-BAVQ is almost the same as WT-VQ and BAVQ. Although WT-BAQ has a shorter run-time, its ASC is smaller in the condition of having smaller CR than WT-BAVQ. Moreover, it is hard to get high CR. When the CR is 64, the magnitude of original image and the decompressed image of these four algorithms are shown in Fig. 5. Fig. 6 gives the magnitude of local amplificatory of original image and the decompressed image. Although the magnitude of the decompressed image which is shown in Fig. 6 has lower quality than the original image, it can keep the phase information effectively. And it can get a compromise in keeping the magnitude and phase information. We can see this conclusion from the ASC and APCC which are shown in Table 1.

Table 1 Comparison of simulation results of four algorithms

	BAVQ	WT-VQ	WT-BAQ	WT-BAVQ
ASC	0.640271	0.612013	0.726567	0.814378
APCC	0.598267	0.631823	0.594736	0.862700
Time/s	165.078	168.235	24.7500	169.953

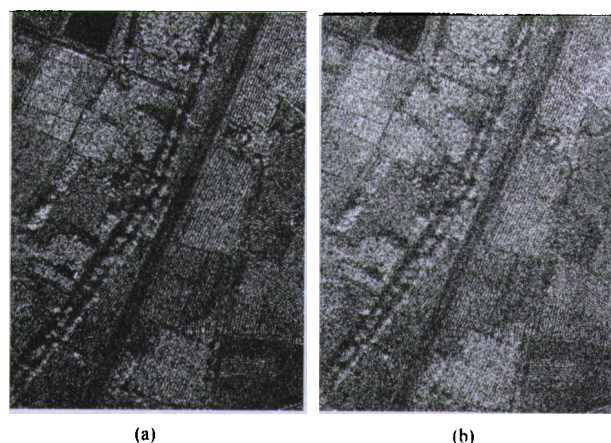


Fig. 5 Magnitude of the original image and the image after decompression

(a) Original; (b) After decompression

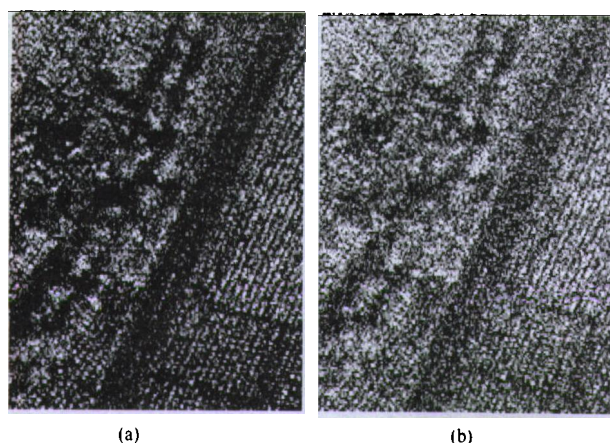


Fig. 6 Magnitude of local amplificatory of original image and the image after decompression

(a) Original; (b) After decompression

7 CONCLUSION

The algorithm proposed in this paper performs vector quantization to SAR complex images in wavelet domain. It makes use of the characteristic that coefficients of SAR complex images are more correlated after the wavelet transform. It also utilizes the correlation between the coefficients in different frequency bands. As a result, it can improve the compression performance. Moreover, because it apply BAQ before vector quantization, the compression time can be shorten at a large extent for generating the codebook only once. BAVQ also has the predominance. As the simulation results show, this algorithm can get high CR as well as keeping the quality of SAR complex images. It is an efficient algorithm. The main work in the future is to find a method which can also keep the magnitude information effectively.

REFERENCES

- Brandfass M, Coster W, Benz U and Moreira A. 1997. Wavelet based approaches for efficient compression of complex SAR image data. *International Geoscience and Remote Sensing Symposium, Singapore*
- Chen S X. 2002. A vector quantization algorithm based on wavelet transforms, *Journal of Chongqing University of Posts and Telecommunications*, 14(1): 87—90
- Eichel P and Ives R W. 1999. Compression of complex-valued SAR images. *IEEE Transactions on Image Processing*, 8(10): 1483—1486
- Ives R W, Magotra N and Kiser C. 1998. Wavelet compression of complex SAR imagery using complex and real-valued wavelets: a comparative study. *Thirty-Second Asilomar Conference. Signals, Systems & Computers*, 2(11): 1294—1298
- Kwok R and Johnson W T K. 1998. Block adaptive quantization of magellan SAR data. *IEEE Transactions on Geoscience and Remote Sensing*, 27(4): 375—383
- Li G G and Jiang W. 2004. Vector quantization based on wavelet-transform and distortion competitive learning. *Information Technology & Informatization*, (6): 21—23
- Linde Y, Buzo A and Gray R M. 1980. An algorithm for vector quantizer design. *IEEE Transactions on Communications*, 28(1): 84—95
- Pan J S, Lu Z M and Sun S H. 2003. An efficient encoding algorithm for vector quantization based on subvector technique. *IEEE Transactions on Image Processing*, 12(3): 265—270
- Qing L, Wang Y F and Hu X X. 2005. An efficient high compression ratio algorithm for SAR raw data. *Journal of Electronics & Information Technology*, 27(8): 1233—1236
- Robert L, Ives R W, Eichel P and Magotra N. 1999. A new SAR image compression quality metric. *Forty-Second Midwest Symposium, Circuits & Systems*, 2(8): 1143—1146
- Wang G Q and Yuan W W. 2001. Generic 9-7-tap wavelets filters and their performances studies on image compression. *Acta Electronica Sinica*, 29(1): 130—132
- Werness S A, Wei S C and Carpinella R. 1994. Experiments with wavelets for compression of SAR data. *IEEE Transactions on Geoscience and Remote Sensing*, 32(1): 197—201
- Zeng Z H and Cumming I G. 2001. SAR image data compression using a tree-structured wavelet transform. *IEEE Transactions on Geoscience and Remote Sensing*, 39(3): 546—552

小波变换块自适应矢量量化压缩 SAR 复图像

丁宏, 易航, 王广学, 黄晓涛

国防科技大学 电子科学与工程学院, 湖南 长沙 410073

摘要: 随着高分辨率合成孔径雷达的快速发展, SAR 系统中所含的数据量越来越大, 必须对大量的复图像数据进行压缩, SAR 复图像数据的压缩不同于 SAR 实图像的压缩, 通常对相位特性的保持要求很高, 所以压缩 SAR 复图像成为研究中的难点。在分析复图像数据经过小波变换后的相关性变化, 研究了使用小波变换块自适应矢量量化 (WT-BAVQ) 压缩合成孔径雷达复图像的理论依据及具体方法。对一幅复图像进行压缩和解压缩, 计算其平均空域相关值和平均相位相关系数, 给出了解压缩之后的图像。与块自适应矢量量化 (BAVQ), 小波变换矢量量化 (WT-VQ), 小波变换块自适应量化 (WT-BAQ) 进行了性能比较。实验结果表明, 在相同压缩比的条件下, 小波块自适应矢量量化算法的平均空域相关值最高。

关键词: SAR 复图像, 小波变换, 块自适应量化, 矢量量化

中图分类号: TP722.6/TP751.1

文献标识码: A

引用格式: 丁宏, 易航, 王广学, 黄晓涛. 2010. 小波变换块自适应矢量量化压缩 SAR 复图像. 遥感学报, 14(1): 033—042
Ding H, Yi H, Wang G X and Huang X T. 2010. Compression of SAR complex image with wavelet transform block adaptive vector quantization. *Journal of Remote Sensing*. 14(1): 033—042

1 引言

随着高分辨率合成孔径雷达的快速发展, SAR 系统中所含数据量越来越大, 由于传输能力的限制, 为了实现 SAR 数据的实时传输必须对其进行压缩, SAR 数据的压缩可分为 3 类: 原始数据的压缩、复图像的压缩和模值图像的压缩。

SAR 复数图像不同于普通的光学图像, 它具有光学图像不具有的 3 种性质: SAR 复图像是带有模值信息和相位信息的复数据; SAR 图像动态范围很大; SAR 复图像中包含丰富的纹理。因此, 很多光学图像的压缩方法不适合 SAR 复图像的压缩。以前, SAR 图像的相位部分被丢弃, 近年来, 很多有效的前沿技术依靠 SAR 数据的复值特性, 例如自聚焦和干涉测量法, 所以, 压缩复图像是非常必要的。目前对于 SAR 复数图像的压缩算法相对较少, 集中在变换域方法, 主要有频率域的压缩 (Eichel & Ives, 1999) 和小波变换域的压缩 (Werness 等, 1994; Brandfass 等,

1997; Ives 等, 1998; Zeng & Cumming, 2001), 频率域压缩复杂度相对较低, 效率不高, 一般压缩比低于 20, 而小波域的压缩算法相反。

考虑到复图像数据实部和虚部经过小波变换后相关性增强的特点, 本文算法将复图像数据分为实部和虚部, 先进行小波变换, 然后对相关性增强的实部和虚部数据进行矢量量化。考虑到复图像数据的分布近似为高斯分布, 作线性变换后, 数据还是近似为高斯分布, 所以在矢量量化前进行 BAQ 压缩, 得到有 N (视 BAQ 量化位数而定) 个幅度的离散高斯分布 (秦蕾等, 2005), 从而整个传输系统的数据具有相同的标准偏差, 矢量量化时只需要一个与数据系统无关的码书, 节省了整个系统的编码时间, 提高了效率。

2 SAR 复图像系数小波分析

对于 $M \times N$ 的数据块, 行间间隔为 k 时的相关系数为:

收稿日期: 2008-10-24; 修订日期: 2009-04-01

基金项目: 教育部新世纪优秀人才支持计划 (编号: NCET-07-0223)。

第一作者简介: 丁宏 (1973—), 女, 讲师, 2001 年于国防科学技术大学电子科学与工程学院获得硕士学位。从事信号处理理论和系统仿真研究, 研究领域包括: 信号检测与估计、SAR 数据处理和无线通信。发表论文近 10 篇, 出版教材 1 部。E-mail: dh1nudt@tom.com。

$$\rho = \frac{\sum_{j=1}^N \sum_{i=1}^M [(X(i, j) - m) \times (X(i+k, j) - m)]}{\sqrt{\sum_{j=1}^N \sum_{i=1}^M (X(i, j) - m)^2} \times \sqrt{\sum_{j=1}^N \sum_{i=1}^M (X(i+k, j) - m)^2}} \quad (1)$$

式中, m 为 $X(i, j)$ 的均值。

列间间隔为 k 时的相关系数为:

$$\rho = \frac{\sum_{i=1}^M \sum_{j=1}^N [(X(i, j) - m) \times (X(i, j+k) - m)]}{\sqrt{\sum_{i=1}^M \sum_{j=1}^N (X(i, j) - m)^2} \times \sqrt{\sum_{i=1}^M \sum_{j=1}^N (X(i, j+k) - m)^2}} \quad (2)$$

式中, m 为 $X(i, j)$ 的均值。

对两幅不同复图像做小波变换前后系数相关性变化的分析。复图像 1 是幅度图如图 1 所示的 P 波段 SAR 复图像, 方位向和距离向的点数均为 1024, 利用双正交 9/7 小波(王和袁, 2001)对图像做三级小波变换, 得到 10 个子带分别为 LL3, LH3, HL3, HH3, LH2, HL2, HH2, LH1, HL1, HH1。利用式(1)和式(2)的定义, 对复图像数据小波变换前后的相关系数在 MATLAB 中进行仿真, 仿真结果如图 2, 其中行表示方位向, 列表示距离向。对一 Ku 波段的 1024×

1024 的复图像 2 作同样处理, 结果如图 3。其中复图像 2 是本文算法仿真实验输入原图, 其幅度图如仿真实验部分所示, 结果如图 3。不难看出, 经过小波变换后, 复图像数据的相关性有所增强, 复图像不同, 数据的相关性增强的程度也不同。

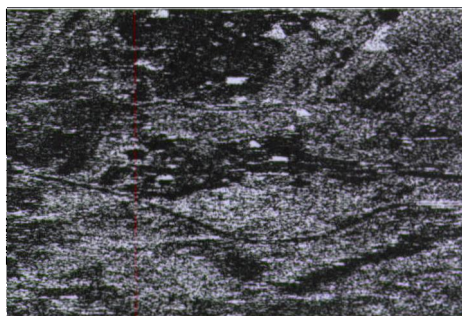


图 1 复图像 1

3 小波系数 BAQ 压缩

SAR 复图像数据可近似为高斯分布, 经过线性变换后, 数据还是近似为高斯分布。本文将 3 层小波变换后的 10 个子带的近似为高斯分布的系数进行 BAQ 压缩(Kwok & Johnson, 1989), 分块大小为

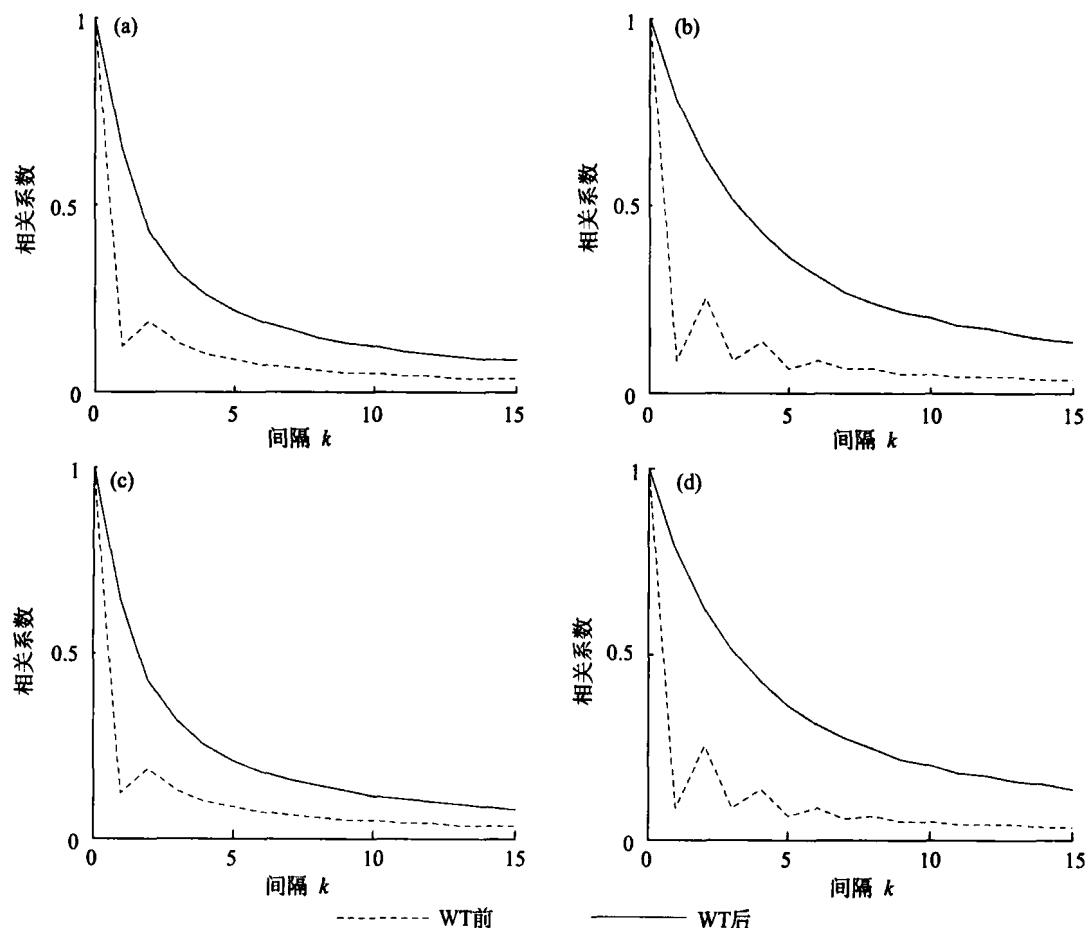


图 2 小波变换前后图像 1 数据的相关系数对比图

(a) 实部方位向上的相关系数; (b) 实部距离向上的相关系数; (c) 虚部方位向上的相关系数; (d) 虚部距离向上的相关系数

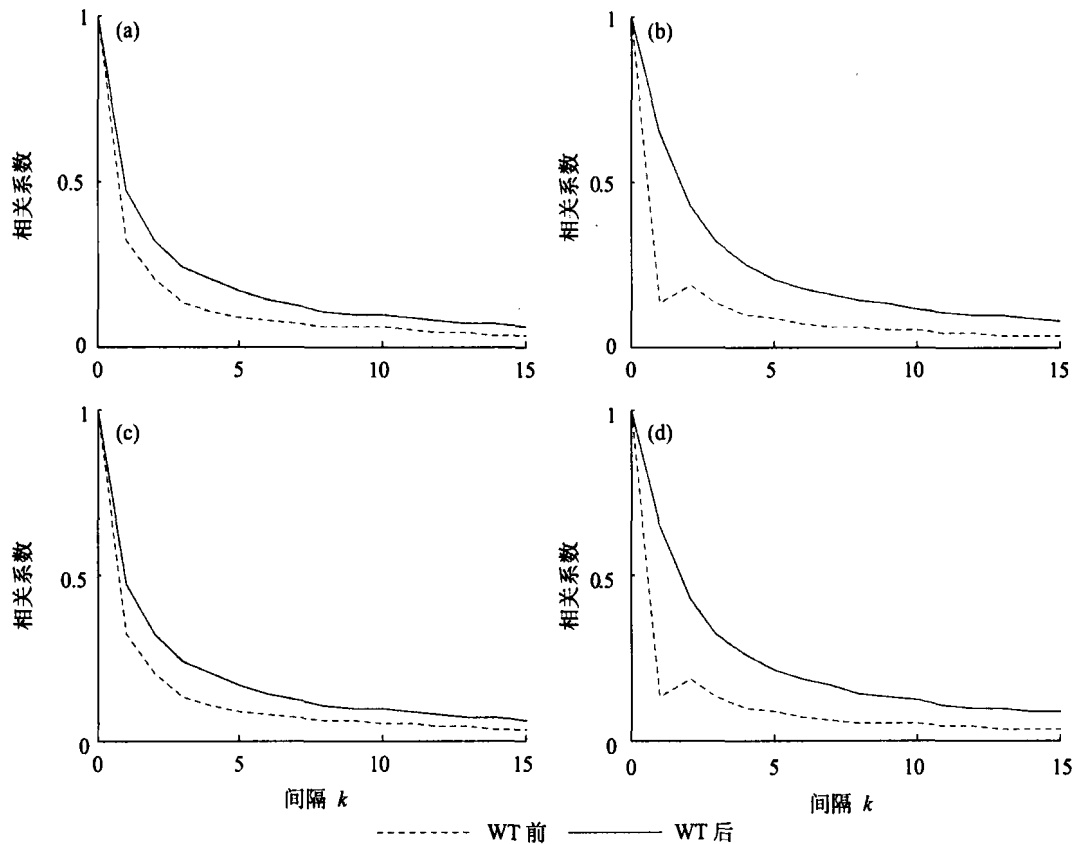


图3 小波变换前后图像2数据的相关系数对比图

(a) 实部方位向上的相关系数; (b) 实部距离向上的相关系数; (c) 虚部方位向上的相关系数; (d) 虚部距离向上的相关系数

32×32。先对每个分块做标准化处理,使均值为0,方差为1。接着根据L-M算法,对标准正态分布的数据做4位量化处理。经过4位BAQ压缩后,得到具有16个幅度离散高斯分布的数据,能够简化后面的矢量量化,因为对于每幅图像,经过小波变换和BAQ压缩后,得到的数据是一样的,所以整个传输系统的数据进行矢量量化时,只需要一个固定的码书,能够有效的节省压缩时间。

4 矢量量化

矢量量化器(Linde等,1980)输入的矢量间的相关性越好,压缩性能越好。已经验证,小波变换后系数之间的相关性有所增强,能提高矢量量化性能。待编码的小波系数的矢量构造,也是编码压缩的一个重要问题,可以决定其后的处理能否简洁高效,对压缩性能也有影响。

4.1 小波系数的矢量构造

采用陈善学(2002)提出的一种方法对BAQ压缩后的小波系数进行矢量构造。小波变换后,高频子带之间存在相当明显的同构特性,这种相似性不仅存在于同一尺度的高频子带内,也存在于不同尺度

的高频子带间,在不同尺度对应频带间的相关性是最强的,要想提高矢量量化的编码效率,必须在构造矢量时充分利用这些相关性。将子带图像中相应的同构像元放在同一矢量中进行量化,是一种直观有效的方法。考虑高频子带的信息在提高重构图像上起着重要作用,矢量构造时包括各种高频子带系数,另外,为避免对低频分量的标量量化,可以和相应的高频系数放在一个矢量中处理。根据上述思想,将不同分辨率下的子图像中对应同一位置的数据按一个树结构结合在一起,生成矢量如图4,这样整个图像可用一个统一的码书。图4是三级小波分解,共10个子带,每级分别取1,4,16个系数,构成

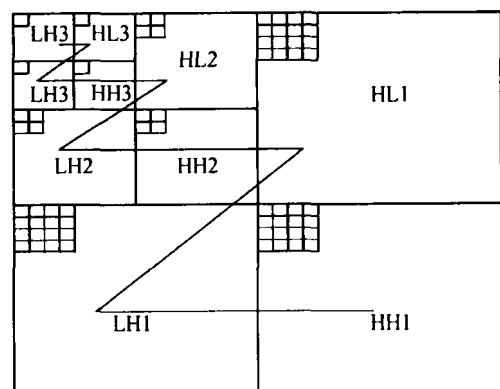


图4 矢量构造

64 维矢量形式(按折线的顺序排列)。文献中, 构造出 64 维矢量后, 采用非线性插补技术生成维数较低的输入矢量进行编码, 考虑到 SAR 复图像的能量分布不集中, 本文直接采用上述方法构造的 64 维矢量编码。

4.2 码书的形成

当输入矢量服从均匀分布时, 采用等概率原则可以得到最优码本; 当输入矢量服从任意分布时, 采用等概率原则不能得到最优码本, 只有采用等误差原则才能得到最优码本。本文的输入矢量不是均匀分布, 利用改进的误差竞争学习算法(李国刚 & 姜伟, 2004)形成码书。

4.3 编码算法

利用输入矢量与码字间的距离特性、码字间的距离特性以及部分失真排除法得到快速矢量量化编码算法。预先计算码书 C 中各个码字和值, 根据递增方式对码书 C 排序, 生成排序码书 C_s , 把和值也保存在码书中, 对于每一个输入矢量计算其和值并利用二分搜索方法寻找与其最近的码字。接着进行往返搜索(Pan 等, 2003), 利用快速矢量量化编码算法的准则完成编码。

5 评估性能指标

本文采用复值空域相关系数(Robert 等, 1999)评估用 WT-BAVQ 压缩 SAR 复图像的性能。

复值空域相关系数(CSCC)定义为:

$$c(x, y) = \frac{\left| \sum_i \sum_j f(i, j) \cdot g^*(i, j) \right|}{\sqrt{\sum_i \sum_j \|f(i, j)\|^2 \cdot \sum_i \sum_j \|g(i, j)\|^2}} \quad (3)$$

式中, 索引值表示像元点 (x, y) 邻域内的像素, 应用式(3)对每个像元点进行邻域求值时, 相关系数落在 $[0, 1]$ 范围内。当原始图像和重建图像在邻域内的每个复数值相等时, 该像元点的相关系数取值为 1.0, 表示两幅图像在该像元点完全相关, 当取值为 0 时意味着完全不相关。上式的应用前提为在邻域内的复数据均值为零。对于复值 SAR 图像, 当邻域尺寸足够大时(例如 5×5), 这样的假设通常是成立的, 本文邻域尺寸取 5×5 。通过计算所有像元点的相关系数值, 可以很直观的知道重建图像和原始图像在邻域内的局部相似程度, 相关系数越大, 意味着重建图像和原始图像的相似程度越好, 如果对整幅图像 $(M \times N)$ 的相关系数求平均值时, 获得了平均空域相关值(ASC):

$$ASC = \frac{1}{MN} \sum_x \sum_y c(x, y) \quad (4)$$

该参数给出了整幅图像平均的相似程度, 可以用来衡量重建图像的全局性能。

对于 SAR 复图像的压缩, 相位特性的保持非常重要, 本文利用平均相位相关系数(Average Phase Correlation Coefficient)对整幅图像的相位保持特性进行分析。借鉴平均空域相关值的定义, 我们定义平均相位相关系数 APCC:

$$APCC = \frac{1}{MN} \sum_x \sum_y \frac{\left| \sum_i \sum_j f_p(i, j) \cdot g_p^*(i, j) \right|}{\sqrt{\sum_i \sum_j \|f_p(i, j)\|^2 \cdot \sum_i \sum_j \|g_p(i, j)\|^2}} \quad (5)$$

式中, $f_p(i, j)$ 和 $g_p(i, j)$ 分别表示原图像及解压之后图像在像元点 (x, y) 处的相位。

6 仿真实验结果分析

待压缩图像是前面所提到的 Ku 波段 SAR 复图像, 方位向和距离向上的点数均为 1024, 幅度图如图 5(a)。分别利用 BAVQ, WT-VQ, WT-BAQ 及 WT-BAVQ 对该复图像进行压缩和解压缩仿真实验, 实验环境为: CPU 为 2GHz, 内存为 2G, Windows XP 操作系统; 程序运行环境: IDL 6.3。表 1 给出了 4 种算法仿真后复图像的平均空域相关值(ASC), 平均相位相关系数(APCC)及运行时间(TIME), 其中 BAVQ, WT-VQ, WT-BAVQ 的码书长度均为 256 (CR=64), 矢量长度为 64, 训练矢量是从所有输入矢量中间隔选取的, 训练矢量长度为所有输入矢量长度的 1/8。BAVQ 和 WT-BAVQ 中的 BAQ 压缩部分采用 4 位 L-M 量化, WT-BAQ 中, 对小波系数进行 2 位 L-M 量化(CR=4)。由表 1 看出, WT-BAVQ 的效果最好, 其压缩比与 WT-VQ, BAVQ 相同, 一次压缩与解压缩过程的运行时间也相当, 但是其平均空域相关值和平均相位相关系数均最大, WT-BAQ 虽然运行时间短, 但是在压缩比远小于 WT-BAVQ 的情况下平均空域相关值也小于 WT-BAVQ, 且 WT-BAQ 很难实现高压缩比。图 5 给出了原复图像及 WT-BAVQ 解压之后的图像, 压缩比为 64。图 6 给出了原图像及解压之后图像的局部放大图。虽然如图 6(b)所示的解压后图像的幅度相对于原图像有一定的损失, 但是由表 1 中计算的平均相关系数和平均空域相关值可知, 本文算法能够有效的保持复图像的相位特性, 并且能在幅度和相位特性的保持上达到折中。

表 1 4种算法的仿真结果比较

	BAVQ	WT-VQ	WT-BAQ	WT-BAVQ
ASC	0.640271	0.612013	0.726567	0.814378
APCC	0.598267	0.631823	0.594736	0.862700
时间/s	165.078	168.235	24.7500	169.953

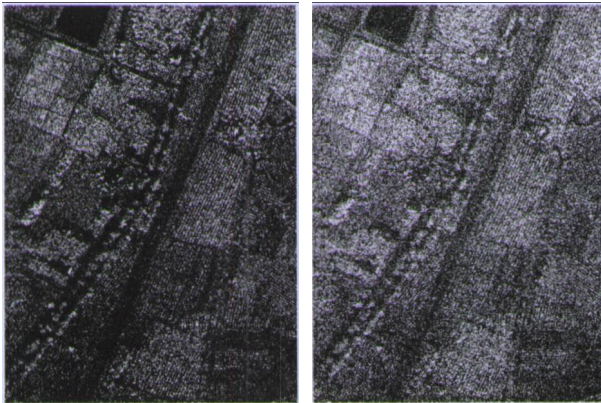


图 5 原图像及解压后的幅度图

(a)原图像; (b)解压后图像

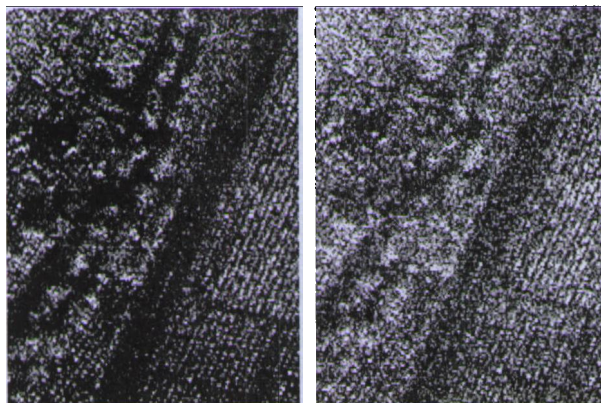


图 6 原图像及解压后图像的局部放大图

(a)原图像; (b)解压后图像

7 结 论

本文算法在小波域对 SAR 复数图像进行矢量量化, 利用复图像数据在小波变换后相关性增强特性以及小波系数的跨频相关性构造矢量量化器的输入矢量, 在构造过程中充分利用了各个频带的系数, 有效地提高了矢量量化的压缩性能, 由于在矢量量化之前采用了 BAQ, 处理之后的结果是具有 16 个幅度的离散高斯分布, 后面的矢量量化所需的码书是相同的, 所以只需要形成 1 次码书, 总的压缩时间可以得到大幅度的减少, BAVQ 同样具有这个优势。实验证明, 该算法在能保证图像质量的情况下实现高压缩比, 是一种有效的算法。下一步的工作是研究如

何提高压缩算法对复图像幅度的保持特性。

REFERENCES

- Brandfass M, Coster W, Benz U and Moreira A. 1997. Wavelet based approaches for efficient compression of complex SAR image data. International Geoscience and Remote Sensing Symposium, Singapore
- Chen S X. 2002. A vector quantization algorithm based on wavelet transforms. *Journal of Chongqing University of Posts and Telecommunications*, 14(1): 87—90
- Eichel P and Ives R W. 1999. Compression of complex-valued SAR images. *IEEE Transactions on Image Processing*, 8(10): 1483—1486
- Ives R W, Magotra N and Kiser C. 1998. Wavelet compression of complex SAR imagery using complex and real-valued wavelets: a comparative study. *Thirty-Second Asilomar Conference. Signals, Systems & Computers*, 2(11): 1294—1298
- Kwok R and Johnson W T K. 1998. Block adaptive quantization of magellan SAR data. *IEEE Transactions on Geoscience and Remote Sensing*, 27(4): 375—383
- Li G G and Jiang W. 2004. Vector quantization based on wavelet-transform and distortion competitive learning. *Information Technology & Informatization*, (6): 21—23
- Linde Y, Buzo A and Gray R M. 1980. An algorithm for vector quantizer design. *IEEE Transactions on Communications*, 28(1): 84—95
- Pan J S, Lu Z M and Sun S H. 2003. An efficient encoding algorithm for vector quantization based on subvector technique. *IEEE Transactions on Image Processing*, 12(3): 265—270
- Qing L, Wang Y F and Hu X X. 2005. An efficient high compression ratio algorithm for SAR raw data. *Journal of Electronics & Information Technology*, 27(8): 1233—1236
- Robert L, Ives R W, Eichel P and Magotra N. 1999. A new SAR image compression quality metric. *Forty-Second Midwest Symposium, Circuits & Systems*, 2(8): 1143—1146
- Wang G Q and Yuan W W. 2001. Generic 9-7-tap wavelets filters and their performances studies on image compression. *Acta Electronica Sinica*, 29(1): 130—132
- Werness S A, Wei S C and Carpinella R. 1994. Experiments with wavelets for compression of SAR data. *IEEE Transactions on Geoscience and Remote Sensing*, 32(1): 197—201
- Zeng Z H and Cumming I G. 2001. SAR image data compression using a tree-structured wavelet transform. *IEEE Transactions on Geoscience and Remote Sensing*, 39(3): 546—552

附中文参考文献

- 陈善学. 2002. 一种基于小波变换的矢量量化算法. *重庆邮电学院学报*, 14(1): 87—90
- 李国刚, 姜伟. 2004. 基于小波变换和误差竞争学习的矢量量化. *信息技术与信息化*, (6): 21—23
- 秦蕾, 王岩飞, 胡晓新. 2005. 一种有效的合成孔径雷达原始数据高倍数压缩算法. *电子与信息学报*, 27(8): 1233—1236
- 王国秋, 袁卫卫. 2001. 一般 9-7 小波滤波器及其图像压缩性能研究. *电子学报*, 29(1): 130—132